

# Synthesis and magnetorheological characteristics of ribbon-like, polypyrrole-coated carbonyl iron suspensions under oscillatory shear

Miroslav Mrlik<sup>a,b</sup>, Michal Sedlacik<sup>a,b\*</sup>, Vladimir Pavlinek<sup>a,b</sup>, Pavel Bazant<sup>a,b</sup>, Petr Saha<sup>a,b</sup>, Petra Peer<sup>c</sup>, Petr Filip<sup>c</sup>

<sup>a</sup> Centre of Polymer Systems, University Institute, Tomas Bata University in Zlin, Nad Ovcirnou 3685, 760 01 Zlin, Czech Republic

<sup>b</sup> Polymer Centre, Faculty of Technology, Tomas Bata University in Zlin, nam. TGM 275, 762 72 Zlin, Czech Republic

<sup>c</sup> Institute of Hydrodynamics, Academy of Sciences of the Czech Republic, Pod Patankou 5, 166 12 Prague 6, Czech Republic

E-mail: *msedlacik@ft.utb.cz*

## ABSTRACT

One of the crucial problems of classical magnetorheological (MR) fluids is their high rate of sedimentation. This disadvantage may be substantially eliminated using core-shell particles. The aim of this study is to prepare spherical carbonyl iron (CI) particles coated with conducting polymer polypyrrole (PPy) with ribbon-like morphology. Their quality and application as a MR material is verified using SEM pictures, FT-IR spectra, oscillatory shear rheometry at different temperatures and concentrations, and measurements of sedimentation stability.

**KEYWORDS** Carbonyl iron; Core-shell; Magnetorheological fluid; Polypyrrole; Viscoelasticity, Ribbon-like particles

## INTRODUCTION

Magnetorheological (MR) fluids are multi-component systems consisting basically of ferromagnetic particles usually within the size range of 100 nm – 10  $\mu$ m in diameter with high magnetic permeability and low levels of magnetic coercivity dispersed in a non-magnetizable medium.<sup>1,2</sup> When a certain external magnetic field strength is imposed, magnetic dipole and multipole moments are induced on each particle because of the multidomain particles' structure. The anisotropic magnetic forces between pairs of magnetized particles promote the structuration into chain-like or columnar particulate structures aligned with the direction of the magnetic field. Such structure development increases the viscosity within the MR fluids by several orders of magnitude and, hence, is able to support shear stresses resulting in large field-dependent viscoelastic moduli and a yield stress generation.<sup>3,4</sup> Moreover, the system returns to initially Newtonian-like fluid again in the absence of an external magnetic field. Such completely reversible, rapid and significant magnetic field-induced structuration enables the use of MR fluids in various active damping systems or torque transducers.<sup>5</sup>

However, the magnetic particles tend to settle rapidly due to their high density compared to that of the suspending medium. The particles' sedimentation consequently affects the efficiency of MR fluids as well as their redispersion. A series of methods have been adopted in the past to improve the low long-term stability of MR fluids, e.g. the addition of various additives (surfactants, thixotropic agents, or fillers), the usage of viscoplastic or stabilized suspending media, or the use of bidispersed or bimorphic MR fluids.<sup>6-8</sup> Recently, core-shell structured particles with a magnetic agent as a core and polymeric layer as a shell have attracted much attention since such particles exhibit decreased density compared to bare magnetic ones. These result in improved long-term stability.<sup>9,10</sup> Simultaneously, the surface layer may also promote the MR effect via better mutual compatibility between particles and the suspending medium.<sup>11</sup>

In the present study, core-shell structured particles with a carbonyl iron (CI) magnetic core and a ribbon-like polypyrrole (PPy) conducting shell were prepared by incorporating in situ polymerization of PPy onto CI particles.<sup>12</sup> Viscoelastic properties as important characteristics reflecting the change of the microstructure within the MR fluid as well as the long-term stability of the prepared system were evaluated.

## **EXPERIMENTAL**

### **Materials**

Carbonyl iron particles (HS grade) greater than 97 % in purity are a product of the BASF company (Germany). Prior to use, pyrrole (Py, 98 %, Aldrich Chemicals, USA) was twice distilled under reduced pressure. The oxidizing agent ammonium persulfate (APS,  $(\text{NH}_4)_2\text{S}_2\text{O}_8$ , 98 %, Aldrich Chemicals, USA) and surfactant cetyltrimethylammonium bromide (CTAB, Lach-Ner, Czech Republic) were used as received.

### **Coating of CI particles with PPy-ribbons**

First, CI particles were treated with 0.5M HCl following the instructions,<sup>13</sup> creating hydroxyl groups on the surface of the particles. The modified particles were then sonicated with the surfactant CTAB water solution for 1 hour. Then, the dispersion of CI particles was transferred to a three-neck flask cooled to 0-5 °C, and monomer Py was added under vigorous stirring. After 20 minutes, the oxidizing agent APS was added in drops. The reaction was carried out for an additional 18 hours.<sup>12</sup>

### **Characterization of prepared particles**

The morphologies of bare CI microparticles and PPy ribbon-like coated ones were studied using a scanning electron microscopy (SEM, VEGA II LMU, Tescan Ltd., Czech Republic), with an operating voltage of 5 kV. FT-IR spectra of the prepared samples were obtained using a Nicolet magna-550 spectrometer, USA, in the range of 4000-700  $\text{cm}^{-1}$ . Further, the magnetic properties of the particles

were examined using a vibration sample magnetometer (VSM, EG&G PARC 704, Lake Shore, USA) at room temperature.

### **Suspension preparation and rheological measurements**

Bare and coated particles were suspended in silicone oil (Dow Corning, Fluid 200, USA,  $\eta \approx 100$  mPa s) with 20, 30, and 40 wt.% particle concentrations. The suspensions were mechanically stirred before each measurement. The viscoelastic properties under an external magnetic field in the range 0-300 mT were investigated using a rotational rheometer Physica MCR501 (Anton Paar GmbH, Austria) with a Physica MRD 180/1T magneto-cell. The true magnetic flux density was measured using a Hall probe, and the temperature was checked with the help of an inserted thermocouple.<sup>14</sup> Rheological measurements at temperatures 25, 45, and 65 °C were performed using a Viscotherm VT2 circulator with a temperature stability of  $\pm 0.02$  °C.

## **RESULTS AND DISCUSSION**

### **Morphology and magnetic properties**

SEM images of the bare CI (a) and coated CI/PPy ribbon-like particles (b) are depicted in Fig. 1. As can be seen, the coating of the CI particles with PPy ribbons does not significantly increase the particle size. The diameter for both bare and coated particles is around one micrometer or less. Moreover, under higher magnification the ribbon-like structures (c) are clearly visible on the surface of CI particles.

The influence of coating on the magnetic properties of CI is presented in Fig. 2. The magnetization curves of bare CI and the core-shell composite show negligible remanence. The magnetization saturation of coated CI/PPy ribbon-like particles is lowered due to the coating of CI with the non-magnetic polymer PPy. However, this slight reduction has no impact on real applications as the values of magnetization of such particles are still sufficient.

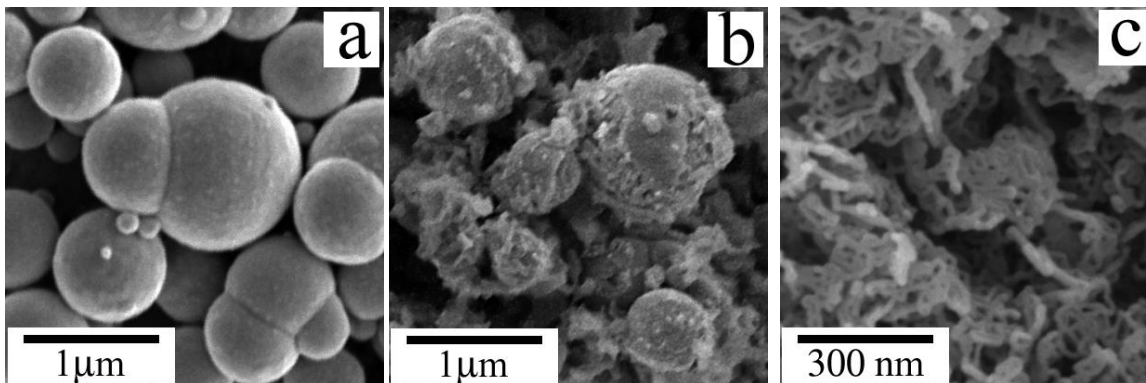


Fig. 1: SEM images of the (a) bare CI particles, (b) CI/PPy-nanoribbons, (c) focused surface of coated CI particle.

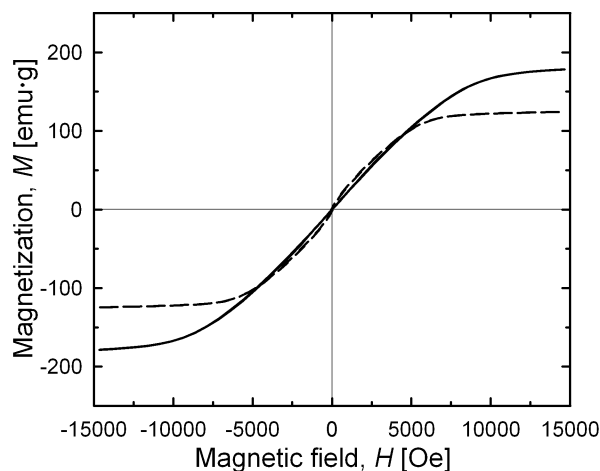


Fig. 2: VSM of bare CI (solid line) and CI/PPy- nanoribbons particles (dashed line)

### Structure characterization

Fig. 3 shows the FT-IR spectra of the bare CI, PPy ribbon-like particles and coated CI/PPy. As expected there are no visible characteristic bands for the bare CI due to their composition >97 % of iron particles. This contrasts to PPy where characteristic bands are as N-H at  $3300\text{ cm}^{-1}$ , C-N at  $1560$  and  $1440\text{ cm}^{-1}$ , and the vibrations related to C-H at  $1240$  and  $1050\text{ cm}^{-1}$ . Strong bands near  $943\text{ cm}^{-1}$  indicate the doping state of PPy.<sup>15</sup> Finally, the successful coating of the bare CI with PPy ribbons is observed in Fig. 3c. The broad band at  $3170\text{ cm}^{-1}$  is related to the N-H stretching mode from PPy. However, the bands become weaker due to bare CI in the CI/PPy ribbon-like system. Furthermore, analogically to the reference<sup>16</sup> some of the vibrations are shifted to lower wave numbers, probably due to the polymerization of the PPy in the presence of the CI particles.

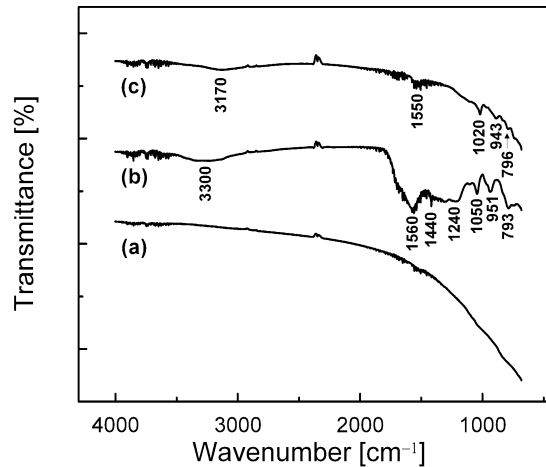


Fig. 3: FTIR spectra of (a) bare CI, (b) PPy ribbon-like particles, and (c) coated CI particles.

### Rheological properties

Generally, MR suspensions are represented by two-phase fluids enabling the transition from a liquid- to solid-like state under application of an external magnetic field. This behaviour is usually examined through measurement in the steady shear mode.<sup>17-21</sup> However, in real applications the MR suspensions are mostly stressed dynamically. This indicates that oscillatory shear measurement is an adequate method for performance evaluation.

Liquid- to solid-like state transition is interlaced with the development of the internal structures when the magnetic field is applied. This behaviour is well documented by the courses of viscoelastic moduli (storage modulus  $G'$  and loss modulus  $G''$ ) and complex viscosity  $\eta^*$  as representative quantities of the dynamic rheological measurement.

An increase of both moduli with increasing magnetic flux density (Fig. 4) implies the formation of internal structures between parallel plates of the rotational rheometer. The plateau for  $G'$  terminates at  $\gamma \sim 3 \times 10^{-4}$ , as for higher values of strain the hydrodynamic forces dominate the magnetic ones. This reflects an irreversible destruction of the internal structures. The plateau indicates the linear viscoelastic region (LVR) in which both moduli are independent of the strain. Further investigation of viscoelastic properties was carried out in the range of strain characterizing the LVR.

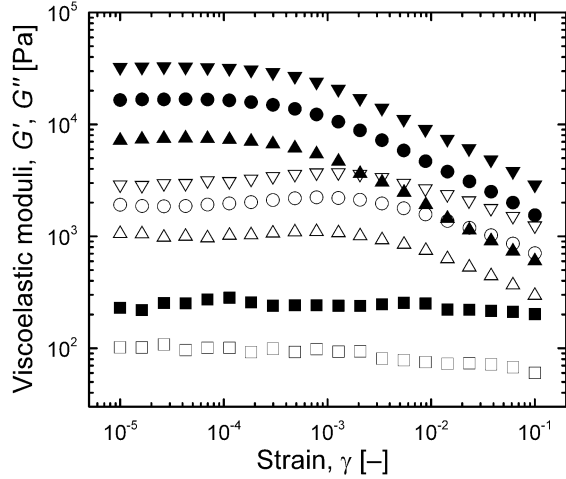


Fig. 4: Dependence of the storage modulus  $G'$  (solid symbols) and loss modulus  $G''$  (open symbols) on the strain  $\gamma$  for 40 wt. % of CI/PPy-nanoribbons in silicone oil, at temperature 25°C, under various magnetic flux density, ( $\square, \blacksquare$ ) 0, ( $\triangle, \blacktriangle$ ) 84, ( $\circ, \bullet$ ) 174, ( $\nabla, \blacktriangledown$ ) 263 mT

The angular frequency dependence of the viscoelastic moduli (Fig. 5) in the absence of the external magnetic field shows elastic behaviour, when  $G'$  is slightly higher than  $G''$ , probably due to higher suspension concentration. In the presence of the magnetic field, both moduli dramatically increase, but  $G'$  dominates  $G''$  in the whole range of the measured angular frequency, indicating relatively stiff three-dimensional structures created by the CI particles coated with PPy ribbons.<sup>22</sup>

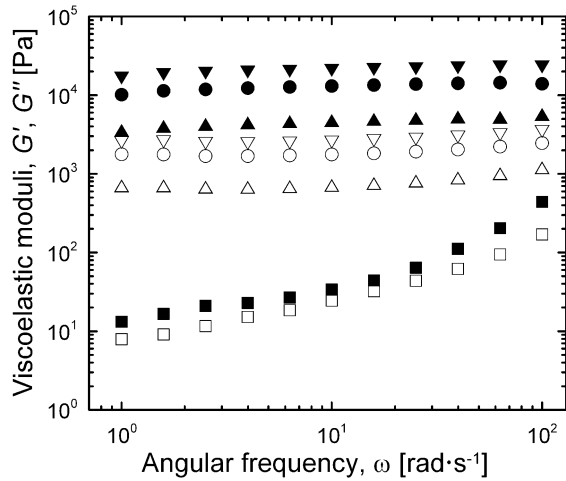


Fig. 5: Dependence of the storage modulus  $G'$  (solid symbols) and loss modulus  $G''$  (open symbols) on the angular frequency  $\omega$ , for 40 wt. % of CI/PPy-nanoribbons in silicone oil, at temperature 25°C, under various magnetic flux density, ( $\square, \blacksquare$ ) 0, ( $\triangle, \blacktriangle$ ) 84, ( $\circ, \bullet$ ) 174, ( $\nabla, \blacktriangledown$ ) 263 mT

Applications of the MR suspension in the industry are usually in coherence with their use at elevated temperatures. Therefore, the investigation of the complex viscosity in the absence (0 mT) and presence (263 mT) of the magnetic field at different temperatures was performed (see Fig. 6). This figure documents a decrease in viscosity of the suspension with increasing temperature both in the absence and presence of an external magnetic field. The viscosity of CI/PPy ribbon-like particle suspensions when the magnetic flux density attains 263 mT, rises over four orders of magnitude in comparison with 0 mT due to the formation of internal chain structures exhibiting similar viscosity values regardless of temperature. Finally, more pronounced shear thinning behaviour was observed due to increasing angular frequency, which contributes to the partial deformation of the structures created in the presence of the external magnetic field.

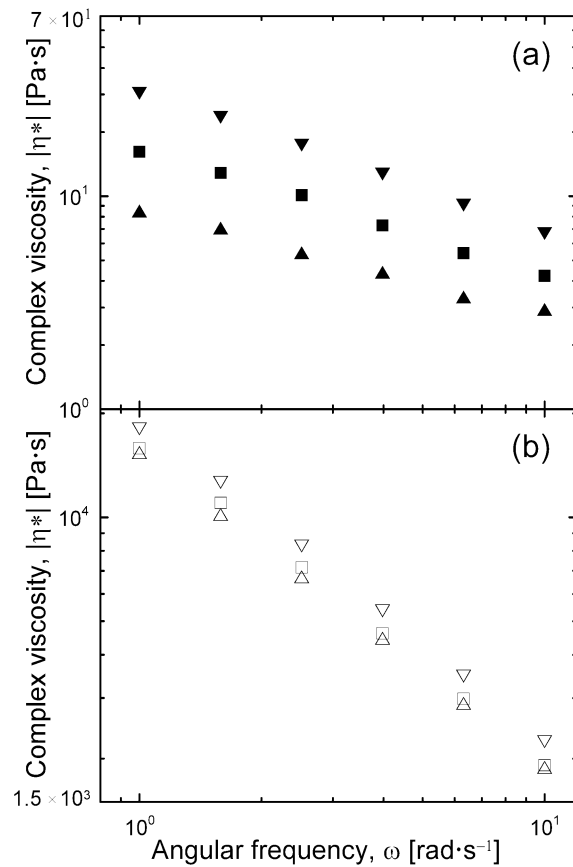


Fig. 6: Dependence of the complex viscosity  $|\eta^*|$ , on angular frequency,  $\omega$ , for 40 wt. % of CI/PPy-nanoribbons in silicone oil in the absence (solid symbols) and in the presence (open symbols) of the magnetic flux density (263 mT) under, at various temperatures, ( $\blacktriangledown \triangledown$ ) 25, ( $\blacksquare \square$ ) 45 and ( $\blacktriangle \triangle$ ) 65 °C.



In order to examine the influence of particle concentration on the MR behaviour under an external magnetic field, the  $G'$  was plotted against the angular frequency  $\omega$  (see Fig. 7). In the absence of the magnetic field, the suspension consisting of 20 wt. % of the coated CI particles attains the lowest values of the elastic modulus. With increasing particle concentration, the  $G'$  increases and a suspension containing 40 wt.% of coated particles reaches the highest values. However,  $G'$  above an angular frequency of about  $30 \text{ rad}\cdot\text{s}^{-1}$  is nearly identical for all samples. High frequency application contributes to an increase in the elastic behaviour of the suspensions. Increase the frequency and shorten the time, and the response to this stimulus results in an enhanced elasticity of the suspensions in comparison to that of a low frequency application indicating mainly viscous behaviour. On the other hand, in the presence of the magnetic field,  $G'$  increases with increasing particle concentration and becomes independent of  $\omega$  in the whole frequency range. This confirms the inherence of strong chain-like structures developed in the suspension.

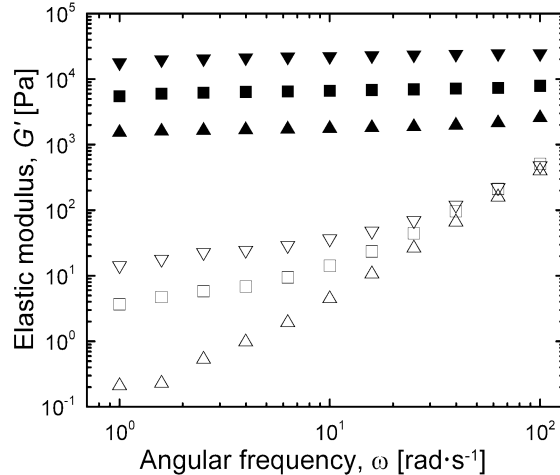


Fig. 7: Dependence of the storage modulus  $G'$ , on angular frequency,  $\omega$ , in the absence (open symbols) and in the presence (solid symbols) of the magnetic flux density (263 mT) at temperature  $25^\circ\text{C}$ , at various concentrations, ( $\blacktriangle$   $\Delta$ ) 20, ( $\blacksquare$   $\square$ ) 30, ( $\blacktriangledown$   $\nabla$ ) 40 wt.% of CI/PPy-nanoribbons in silicone oil.

The dependence of the viscoelastic moduli on the magnetic flux density (Fig. 8) proves the good MR behaviour of the prepared material. The viscoelastic moduli of both materials, CI and coated CI with PPy ribbons, increase with increasing magnetic flux density. The partially lower values of the viscoelastic

moduli for the suspensions with CI/PPy ribbon-like particles in comparison with bare CI are more than balanced out by their much better sedimentation stability as shown below.

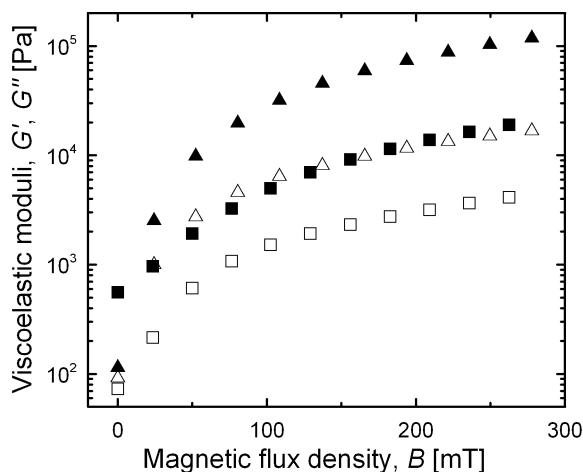


Fig. 8: Dependence of the storage modulus  $G'$  (solid symbols) and loss modulus  $G''$  (open symbols) on the magnetic flux density,  $B$  for 40 wt. % fraction, at temperature  $25^\circ\text{C}$ , where (■ □) are CI/PPy-ribbons, (▲ △) are bare CI.

### Sedimentation stability

Sedimentation is a key factor influencing the use of MR suspensions in many applications. The sedimentation test measured by naked-eye method reveals that the stability of bare CI particle suspension is insufficient (Fig. 9). On the other hand, with the PPy ribbon-like structures synthesized on the surface of CI, the sedimentation stability increases and the particles showed stable behaviour during the 30-hour test. The polymer coating on the CI particles with PPy ribbons partially decreases the particle density and probably increases the particle-silicone oil interactions<sup>22</sup> that contribute to the enhancement of the sedimentation stability.

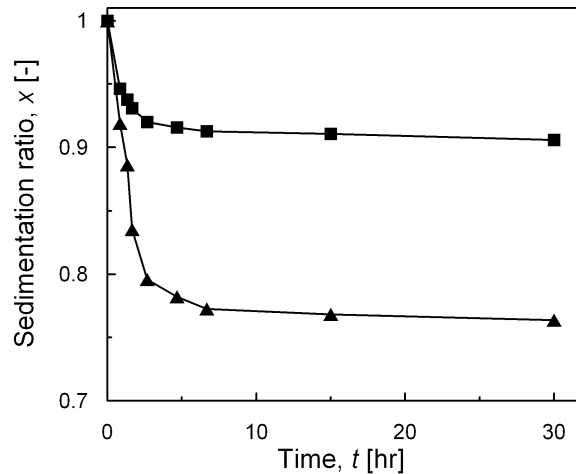


Fig. 9: Sedimentation ratio of 40 wt. % particles in silicone oil at temperature 25°C, where ▲ are bare CI and ■ are CI/PPy nanoribbons.

## CONCLUSIONS

A simple way to prepare coated CI particles with PPy ribbons was presented. CI/PPy ribbon-like particles showed lower magnetization saturation in comparison with bare CI particles due to the coating of the surface with a non-magnetic polymer. Further, the MR efficiency of the suspension of coated CI rapidly increases with increasing temperature. This efficiency is lower than that of suspensions of bare CI particles, nevertheless, the sedimentation stability of the suspension with coated particles is enhanced and stable for tens of hours whereas the suspension consisting of bare CI rapidly decreases within the same time period.

## ACKNOWLEDGEMENTS

This article was written with the support of Operational Program Research and Development for Innovations co-funded by the European Regional Development Fund (ERDF) and national budget of the Czech Republic, within the framework of the project of the Centre of Polymer Systems (reg. number: CZ.1.05/2.1.00/03.0111). The authors further thank the internal grant of TBU in Zlin No. IGA/1/FT/11/D funded from specific university research resources.

## REFERENCES

1. de Vicente, J.; Klingenberg, D. J.; Hidalgo-Alvarez, R. *Soft Matter* **2011**, *7*, 3701-3710.
2. Park, B. J.; Fang, F. F.; Choi, H. J. *Soft Matter* **2010**, *6*, 5246-5253.
3. Bica, I. J. *Ind. Eng. Chem.* **2006**, *12*, 501-515.
4. Bossis, G.; Lacis, S.; Meunier, A.; Volkova, O. *J. Magn. Magn. Mater.* **2002**, *252*, 224-228.
5. Wang, D. H.; Liao, W. H. *Smart Mater. Struct.* **2011**, *20*, 023001
6. Fang, F. F.; Choi, H. J.; Jhon, M. S. *Colloid Surf. A-Physicochem. Eng. Asp.* **2009**, *351*, 46-51.
7. Lopez-Lopez, M. T.; de Vicente, J.; Gonzalez-Caballero, F.; Duran, J. D. G. *Colloid Surf. A-Physicochem. Eng. Asp.* **2005**, *264*, 75-81.
8. Wereley, N. M.; Chaudhuri, A.; Yoo, J. H.; John, S.; Kotha, S.; Suggs, A.; Radhakrishnan, R.; Love, B. J.; Sudarshan, T. S. *J. Intell. Mater. Syst. Struct.* **2006**, *17*, 393-401.
9. Fang, F. F.; Choi, H. J.; Choi, W. S. *Colloid Polym. Sci.* **2010**, *288*, 359-363.
10. Fang, F. F.; Choi, H. J.; Seo, Y. *ACS Appl. Mater. Interfaces* **2010**, *2*, 54-60.
11. Sedlacik, M.; Pavlinek, V.; Saha, P.; Svrčinova, P.; Filip, P.; Stejskal, J. *Smart Mater. Struct.* **2010**, *19*, 115008.
12. Zhang, X. T.; Zhang, J.; Song, W. H.; Liu, Z. F. *J. Phys. Chem. B* **2006**, *110*, 1158-1165.
13. Belyavskii, S. G.; Mingalyov, P. G.; Giulieri, F.; Combarrieau, R.; Lisichkin, G. V. *Protect. Met.* **2006**, *42*, 244-252.
14. Laun, H. M.; Gabriel, C. *Rheol. Acta* **2007**, *46*, 665-676.
15. Cheng, Q. L.; He, Y.; Pavlinek, V.; Li, C. Z.; Saha, P. *Synth. Met.* **2008**, *158*, 953-957.
16. Somani, P. R.; Marimuthu, R.; Mulik, U. P.; Sainkar, S. R.; Amalnerkar, D. P. *Synth. Met.* **1999**, *106*, 45-52.
17. Kim, I. G.; Song, K. H.; Park, B. O.; Choi, B. I.; Choi, H. J. *Colloid Polym. Sci.* **2011**, *289*, 79-83.
18. Liu, Y. D.; Fang, F. F.; Choi, H. J. *Colloid Polym. Sci.* **2011**, *289*, 1295-1298.
19. Lopez-Lopez, M. T.; Kuzhir, P.; Meunier, A.; Bossis, G. *J. Phys.-Condes. Matter* **2010**, *22*, 324106.
20. Sedlacik, M.; Pavlinek, V.; Lehocky, M.; Mracek, A.; Grulich, O.; Svrčinova, P.; Filip, P.; Vesel, A. *Colloid Surf. A-Physicochem. Eng. Asp.* **2011**, *387*, 99-103.
21. Shambharkar, B. H.; Umare, S. S. *J. Appl. Polym. Sci.* **2011**, *122*, 1905-1912.
22. Tsuda, K.; Takeda, Y.; Ogura, H.; Otsubo, Y. *Colloid Surf. A-Physicochem. Eng. Asp.* **2007**, *299*, 262-267.